

Design of an Addressable Internetworked Microscale Sensor

Kyle Yench, Matthew Zofchak, Daniel Oakum, Gerre Strait, Baris Taskin and Bahram Nabet

Abstract—The use of nanoscale structures in sensing applications has been heavily investigated in recent years, with many significant breakthroughs that suggest a bright future for the technology. Silicon nanowires have received particular attention for their use as sense elements because of their large surface area-to-volume ratios and ability to be chemically altered to facilitate the binding of chemical or biological agents. The binding of these agents induces a conductance change in the wire, which can be monitored to detect the presence of trace amounts of an agent in a sample. The goal of the Addressable Internetworked Microscale Sensor (AIMS) system is to design a lab on a chip capable of detecting these small changes in conductance, and transmitting the data for analysis. The Complementary Metal Oxide Semiconductor (CMOS) integrated circuit is a 1.5mm by 1.5mm chip built in AMI C5F 0.5 μ m technology with a 4×4 array of nanowire sensors. A response time of 30 μ s is measured with a tunability of 100k Ω to 100M Ω in nanowire resistance for sensitivity to external binding agents.

Index Terms—Embedded, Lab on a chip, Amplifier, Nanowire, Sensor.

I. INTRODUCTION

SILICON nanowires [1–3], when properly coated to detect a specific agent, present the potential to be harnessed as a new, accurate, real time sensing mechanism. Much research toward implementing this technology has been done by C. Lieber et. al [4]. Lieber’s work details how a protein binding to a coating on the outside of a silicon nanowire changes its conductance as depicted in Figure 1 [4]. Part A in Figure 1 demonstrates the binding of a protein to the silicon nanowire labeled SiNW. The surface of the nanowire is coated with a receptor designed to interact only with a specific molecule. When this interaction occurs, the target molecule binds to the receptor, inducing a conductance change in the wire. By monitoring the nanowire conductance in real-time, the presence of biological and chemical molecules within a sample can be detected. These sensors are able to detect lower concentrations than current sensing methods, down to the level of single viruses [5, 6]. The response time is measured in micro seconds, varying for various receptor types and concentrations. Utilizing nanowires as sensing mechanisms stands to improve time-to-result over conventional detection practices and offers exciting opportunities as a lab-on-a-chip system.

The future work that Lieber recommends in [4] is the construction of an array of nanowire sensing sites. That is

Kyle Yench, Matthew Zofchak, Daniel Oakum and Gerre Strait were with the Department of Electrical and Computer Engineering, Drexel University, Philadelphia, PA 19104 while performing this work.

Baris Taskin and Bahram Nabet are with the Department of Electrical and Computer Engineering, Drexel University, Philadelphia, PA 19104 USA (E-mails: {taskin, nabet}@coe.drexel.edu).

the focus of this paper. The goal is fabrication of an electrical platform ready for active nanowires. The system also includes a complete datapath, including a graphical interface to present results to the users. The presented Addressable Internetworked Microscale Sensor (AIMS) entails the integration of a 4×4 array of functionalized nanowire contact sites on Complementary Metal Oxide Semiconductor (CMOS) circuitry integrated with CMOS amplification circuitry. AIMS design also entails a Printed-Circuit Board (PCB) based data acquisition system to establish communication between the CMOS integrated circuit sensor and a computer system through a Graphical User Interface (GUI) to plot and demonstrate the detected agents. The AIMS device can detect a conductance change on a nanowire and report the characterized data based on the type of coating using the conductivity change, which can be reconfigured for repeated use on different agents or concentrations.

The rest of this paper is organized as follows. In Section II, the operation of the nanowire sensor designed in [4] is briefly reviewed. In Section III, related work on nanowire-based sensors is reviewed. In Section IV, the CMOS integrated circuit design with the nanowire integration to the 4×4 sensor platform and the amplification circuitry is presented. In Section V, the PCB board design to couple with the proposed CMOS integrated circuit design is briefly described. In Section VI, the testing and measurement results of the AIMS design are presented, particularly pertaining to the CMOS integrated circuit component. Finally, conclusions are offered in Section VII.

II. NANOWIRE SENSOR

In [4], the deposition of nanowires (NWs) of semiconducting silicon (Si) as sensors has been presented. The semiconducting Si nanowires can be coated to detect a specific agent by binding to the agent. The binding event changes the conductivity of the semiconducting nanowire element. At the simplest setting, the change in the nanowire conductivity is processed via a CMOS field-effect transistor (FET) to which the nanowire is connected. The conductivity change triggers a switching event at the transistor, which is registered as the detection of the agent, establishing the sensing mechanism.

Demonstrated in Figure 1 [4] is the detection of protein molecules on a silicon nanowire at varying sensitivity ranges. Parts B, C, D and E in Figure 1 demonstrate this conductance change for various levels of the receptor (biotin), which is the activation agent of the nanowires. In particular, the nanowire in Part B is activated less than the nanowires in Parts D

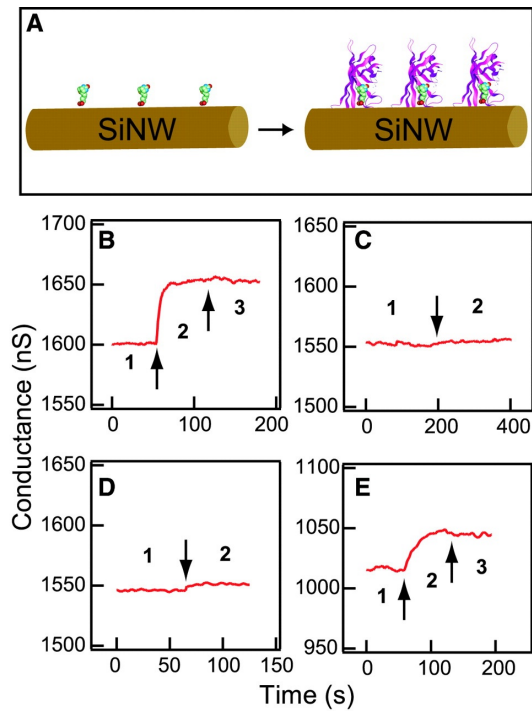


Fig. 1. Nanowire conductance change with protein binding [4].

and Parts E (thus the nanowires in Parts D and E are more sensitive). The nanowire in Part C is not activated at all. Nanowires in all experiments are exposed to the same binding agent (250 nm streptavidin). The regions marked 1, 2, and 3 denote the states of conductance in the nanowire over time as a protein binds to a receptor. Region 1 is before the binding event, which is the addition of a buffer solution. Region 2 corresponds to the addition of the binding agent (250nm streptavidin). Region 3 corresponds to the addition of a pure buffer solution.

It is observed in Part B that the conductivity of the nanowire changes quickly (mark 1) upon the addition of the binding agent. Thus, the detection of the agent is very fast. Part C demonstrates that the same reaction is not observed for nanowires that are not activated. The activation level of each nanowire can be changed in order to change the sensitivity to the level of binding agent as well. In Parts D and E, it is observed that sensitivity to the presence (binding) of the agent is established at a much lower conductivity level. These experiments in [4] demonstrate that nanowire sensors provide fast and high-resolution (down to the level of single viruses) sensing mechanisms. The change in conductivities are maintained after the addition of the pure buffer solution (mark 3). Equally importantly, as the activation agent can be replaced (e.g. washed off with another buffer buffer solution and reapplied), the same nanowire sensor can be *reconfigured* for varying levels or types of agents.

III. RELATED WORK

The scientific work on nanowire-based sensors require advancements in two frontiers: The controlled fabrication of nanowires and the microelectronic system design for detection

resolution and processing. The use of nanowires has recently been investigated for a number of sensing applications such as chemical and biological sensing, including the sensing of biomolecules presented in this paper [4, 7–11]. In the majority of these papers advocating the use of nanowires for sensing, the binding advantage is the level of resolution achievable with nanowires, as with proper fabrication, the surface to volume ratio can be very favorable and the nanostructure enables very resolution sensing.

Circuitry to detect the sensing activity on an integrated circuit environment is a relatively common affair. The literature on sensors and actuators include a myriad of different implementations for read-out circuitry. The critical importance of read-out circuitry is in the design art itself. The presented nanowire-CMOS sensor design encapsulates a tunable range amplifier, which is specific to the designed application. The ability to electrically tune the output voltage range of the amplifier in the read out circuitry enables dynamic tuning of the nanowire-sensor for different chemical agents.

IV. NANOWIRE-CMOS SENSOR DESIGN

The nanowire-CMOS sensor design of the AIMS system includes the design of the sensor sites for nanowire growth (deposition) and the read-out circuitry. The layout of the sensor site is presented in Figure 2. In order to deposit the

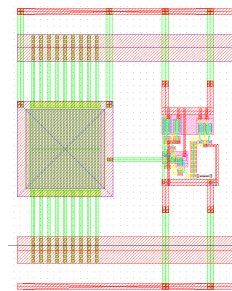


Fig. 2. Integrated circuit sensor site.

nanowires, microfluidic channels [12, 13] are deposited above the presented sensor sites. These microfluidic channels serve to facilitate the deposition of nanowires to the contact pads of the CMOS FETs. The channels also serve to deliver a chemical sample to the sensor sites for analysis. The silicon nanowires themselves are pulled to the sensor sites using a dielectrophoresis [14]. The dielectrophoretic system provides the wires to be moved to the sites by a differential voltage gradient delivered on a metal layer below the landing pads themselves. The contact process is completed by gold contact deposition.

Through simulation, the effective delay from the nanowire site to the output bond pads is measured to be 45 nanoseconds. This low delay value allows the platform to log a substantial amount of data pertaining to the condition of the nanowire.

The CMOS IC platform of the AIMS system contains a current mirror [15, 16], a transimpedance amplifier [15, 16] and a common-source amplifier [15, 16]. This circuitry, schematic of which is shown in Figure 3, is called the amplification stage and serves as the read-out platform for the nanowire

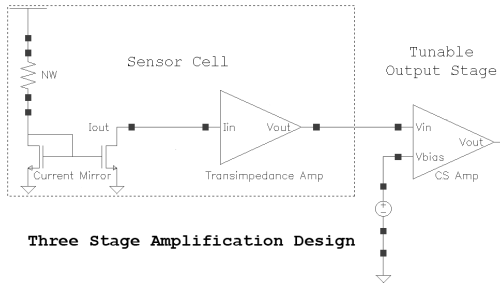


Fig. 3. Schematic of the amplification stage circuitry with three stages: 1) The current mirror and 2) The transimpedance amplifier in the sensor cell and 3) The current source amplifier constituting the tunable output stage.

site. The amplification stage circuitry performs the tasks of the amplification of current changes on the line, translation of the current change to a change in voltage and an adjustable-bias amplifier to drive the signal to the IC outputs, performed at the three stages shown in Figure 3, respectively. The landing pads of the nanowires are connected to the power source and their outputs are connected to the current mirror in order to copy the induced current to the transimpedance amplifier. This circuit converts the change in current caused by binding events on the nanowires to changes in voltage. The schematics of the current mirror and the transimpedance amplifier are shown in Figure 4.

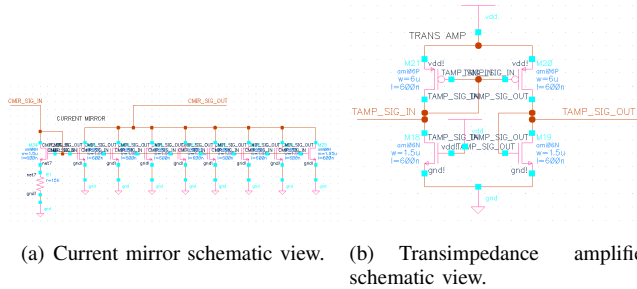


Fig. 4. The current mirror and the transimpedance amplifier in the amplification stage circuitry of the sensor cell in Figure 3.

The final stage of amplification takes place at the common-source (CS) amplifier, which boosts the voltage change from the transimpedance amplifier, in the millivolts range, up to a signal in the $0-V_{DD}$ volt range. The schematic and layout of the current source amplifier stage are shown in Figure 5. The current source amplifier stage is built with tunability, such that,

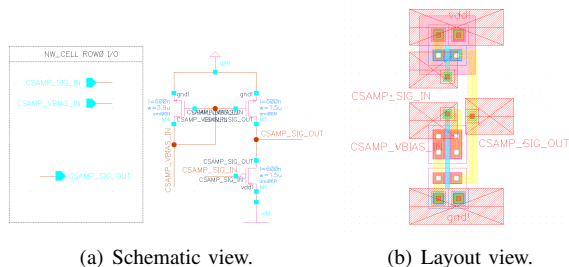


Fig. 5. The design of the current source amplifier (Tunable Output Stage) in the amplification stage circuitry in Figure 3.

by applying a bias voltage ($CSAMP_VBIAS_IN$ in Figure 5), the gain factor of the amplifier can be changed. The tunability is used in order to read-out the conductance change of the nanowires for varying binding agents. Note that the same nanowire sensors can be used in order to detect different agents by replacing the receptors on these wires. The receptors are replaced with a chemical process that does not require the remanufacturing of the chip or the regrowth of the nanowires, thus the same AIMS system can be reused for detection of different agents. This is illustrated through simulations with varying resistance of the nanowires in Figure 6. In Figure 6(a), the range of currents detected from the nanowire of resistances between $1k\Omega$ up to $1M\Omega$. This current is amplified through the transimpedance and the common source amplifiers. The output voltage at the tunable stage of the common source amplifier is presented in Figure 6(b). For nanowire resistances in the $1k\Omega$ up to $1M\Omega$ range, and with the bias voltage $CSAMP_VBIAS_IN$ changing between V_{DD} and $0.75V_{DD}$, the output voltage varies between 0 and V_{DD} . As observed in Figure 6(b), the output voltage level can change on the order of volts over $100k\Omega$ of nanowire resistances by changing the bias voltage.

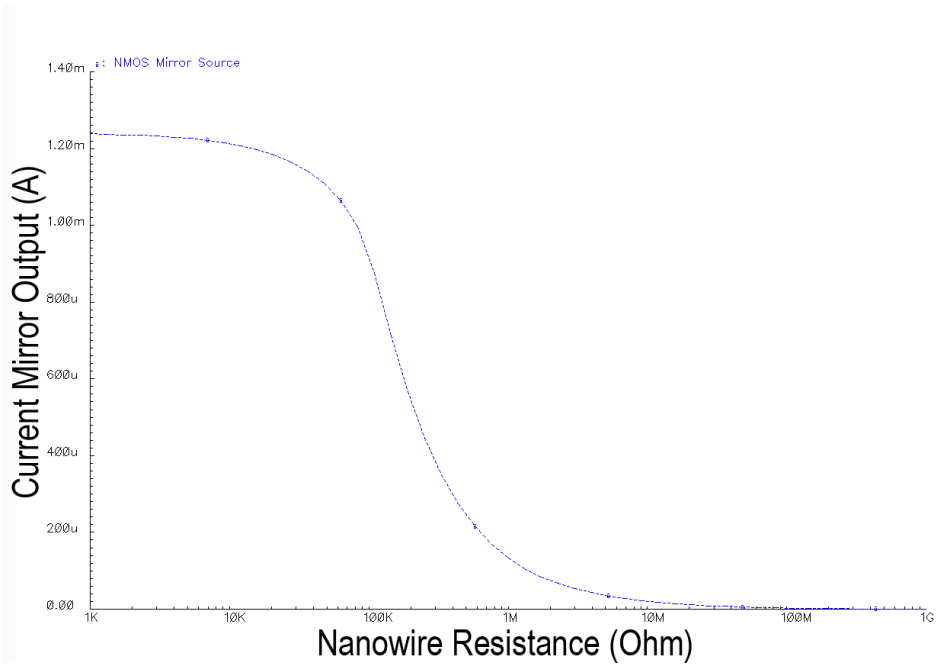
V. DATA ACQUISITION DESIGN

The AIMS system also integrates a communication system that translates the analog voltage from the sensor sites into a digital output. The main tasks of this system are configuring each sensor site, reading data from each sensor site and transmitting collected data to the GUI [17]. Key components of this data acquisition sub-system are the analog-to-digital controllers (ADCs) and the DS80C400 Network microcontroller [18]. The microcontroller is responsible for collecting data from all the ADCs and transmitting it to the GUI. Every sense site requires analog to digital conversion but providing it at each cell level causes unnecessary overhead in area and power. In the presented design, the outputs of each four (4) sense sites (of the 4×4 sensor arrays) are multiplexed over four (4) ADCs. This creates a requirement that the ADCs sample at a sufficiently high frequency such that no data from any input could be missed.

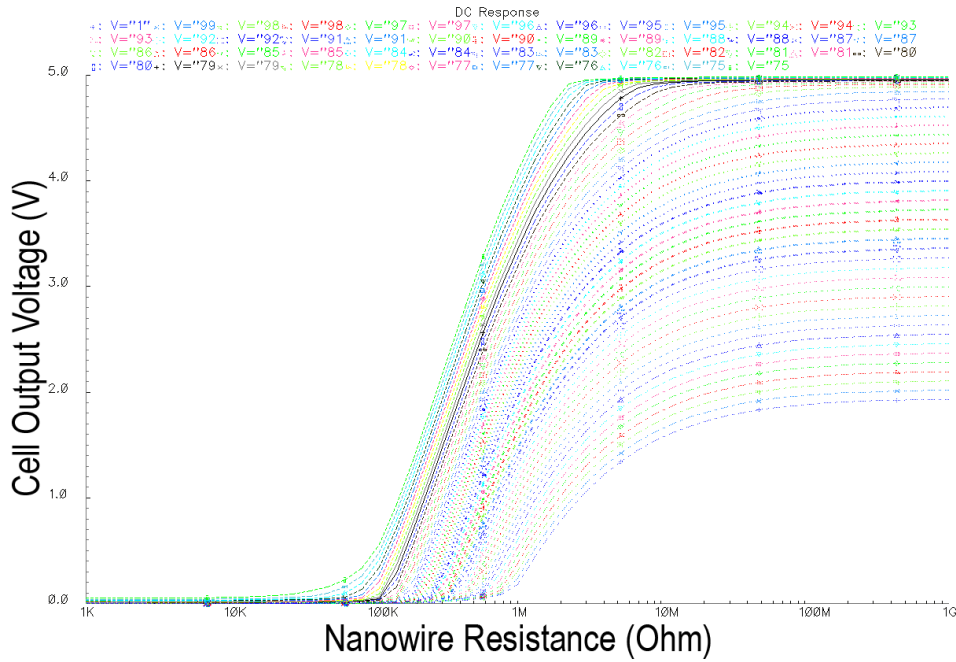
It is possible that amplifiers need to be adjusted for optimal output for different types of active nanowires. To accommodate this, when the microcontroller changes the input to each ADC, it uses the bus for ADC input to quickly output a digital reference that tunes the bias voltage for that particular sense site. The microcontroller is required to store this value for each sense site but it ensures that clipping or saturation will not effect valid data. The deficiency of the number of I/O pins on the DSTINI-KIT board (used with the DS80C400 microcontroller) is addressed by populating the development board with a Xilinx Coolrunner-2 CPLD [19]. This configuration allows for a multiplexed array of 32 GPIO's.

VI. EXPERIMENTAL RESULTS

The prototype chip was fabricated through the MOSIS service [20], on AMI Semiconductor's (now ON Semiconductor) 0.5-micron C5F process scale at $1.5mm\times 1.5mm$ dimensions.



(a) Current mirror output for varying nanowire resistances.



(b) Common-source amplifier output for varying bias voltages.

Fig. 6. Simulation of the amplifier output stages shown in Figure 3.

The IC is wirebonded to a lead frame in house in order to allow testing. The final chip design is shown in Figure 7. The total average power dissipation of the circuit is rated at $120mW$.

Several tests have been conducted to verify the operation of the fabricated AIMS IC against simulations. In particular, the settling (response) time of the nanowire sensor and the sensitivity to nanowire resistance changes due to varying agent densities and types are recorded. The settling time for a binding event is measured between the time required for the output to stabilize when the sense cell input multiplexer is

triggering between an unbound and bound resistance value. A $30 \mu s$ settling time is shown in Figure 8. This settling time is larger than the (pre-silicon) simulated value due to the off-chip capacitances driven by the output stage resistors. Nevertheless, a very fast settling time in the microseconds range is measured.

The sensitivity of the AIMS system to nanowire resistance changes due to effects of varying agents has been characterized. For this purpose, nanowire sensor array output is bypassed to be driven by auxiliary off-chip resistors instead. The

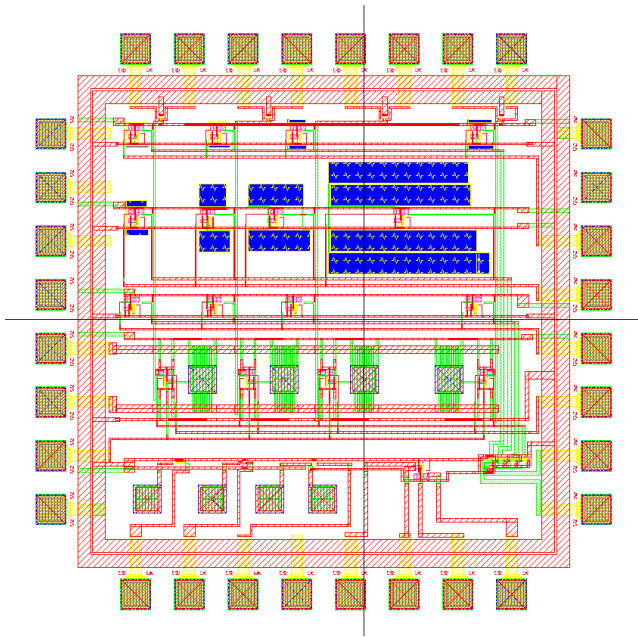


Fig. 7. Integrated circuit sensor layout at $1.5\text{ mm} \times 1.5\text{ mm}$.

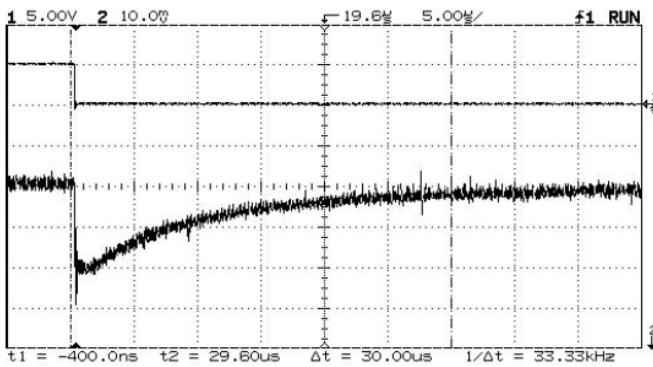


Fig. 8. Settling (response) time of $30\ \mu\text{s}$ of the sensor cell to nanowire resistance change in the presence of a binding event.

resistances are selected to have a range of values representative of the conductance change due to nanowires detecting varying levels and types of agents. These auxiliary resistances provide a more controllable environment for testing the prototype device, which is an alternative of appropriating various agents and receptors for reconfigurability. Naturally, in a production design of this lab-on-chip [13], a more thorough analysis with biological and chemical agents is necessary.

In order to perform this sensitivity characterization using the auxiliary resistors, parametric sweeps on the cell input (nanowire) resistance and the tunable output stage transistors are performed. The results of the sensitivity analysis is shown in Figure 9. Figure 9(a) depicts the simulated and measured responses of two resistances ($500\text{k}\Omega$ and $550\text{k}\Omega$). The simulated traces are the two curves on the left (one for each resistance value) whereas the measured traces are the ones on the right. Consider the following scenario for this analysis: Assume that in the absence of a known, targeted agent, the nanowire has a resistance equivalent of $500\text{k}\Omega$. When the agent

binds to the nanowire, the equivalent resistance changes to $550\text{k}\Omega$. Targeting to detect such resistance-equivalent values, the designed CMOS circuitry is calibrated by setting the output stage bias voltages (x-axis value) such that the tunable amplifier output (y-axis value) is 2.5V for an equivalent resistance of $500\text{k}\Omega$. The tunable amplifier output calibration line is the horizontal threshold line in Figure 9(a).

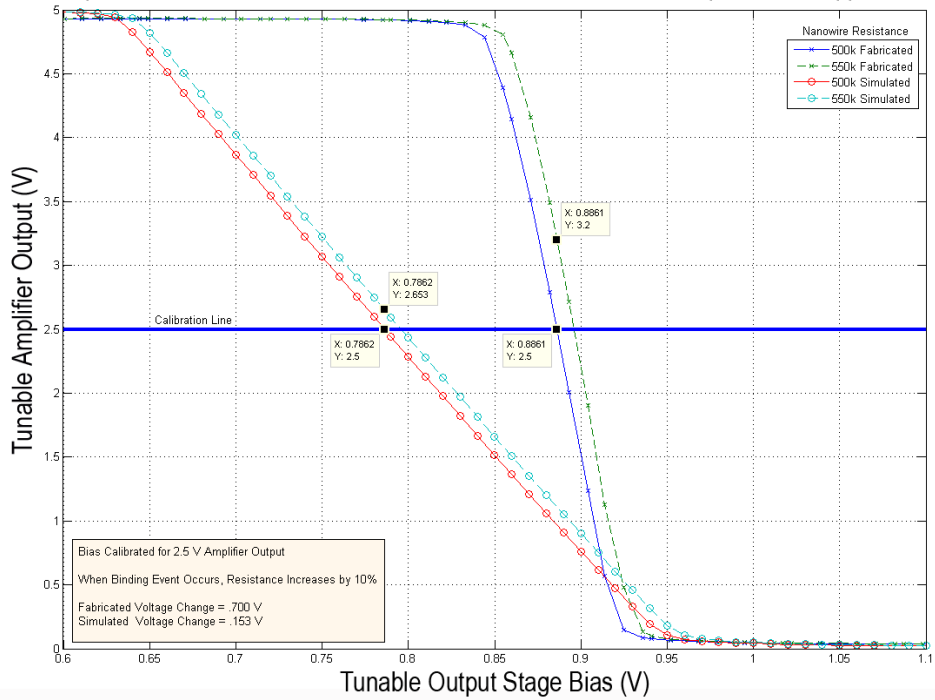
In the pre-silicon simulated responses (two curves on the left), when the agent binds to the nanowire, that is, when the resistance increases from $500\text{k}\Omega$ to $550\text{k}\Omega$, the tunable amplifier output (y-axis value) changes from 2.5V to 2.653V for the selected, fixed output stage bias voltage of 0.7862V (x-axis value). Thus, it is expected from simulations that the detection of the agent would cause a voltage change of approximately $2.653 - 2.5 = 0.153\text{V}$. This change is demonstrative of one of the highest resolutions of the nanowire-based sensor; for higher resistance changes, higher voltage swings are observed. In the post-silicon measurements (two curves on the right), the tunable amplifier output (y-axis value) changes from 2.5V to 3.2V for the same stimulus and the selected, fixed output stage bias voltage value of 0.8861V (x-axis value). The detection of the same agent, thus, actually causes a significant voltage change of $3.2 - 2.5 = 0.7\text{V}$. The discrepancy is due to the resistance and capacitance of the bond wires. These parasitics cause a small voltage drop between the second and third amplification stages (Figure 3), trading the range of valid nanowire sensors for increased sensitivity. Nevertheless, the post-silicon measurement results prove to be superior to the pre-silicon simulated results, improving the operational characteristics of the nanowire-sensor based AIMS system.

The sensitivity experiments are repeated for nanowire resistances in the $100\text{k}\Omega$ to $100\text{M}\Omega$ range and the resulting plot of measured data is shown in Figure 9(b). The high tunability of the output stage is observed for nanowire resistances of up to $5\text{M}\Omega$. The tunability of the output stage staggers for nanowire resistances above this value, yet demonstrates the exceptional sensitivity for all values in range of $100\text{k}\Omega$ to $100\text{M}\Omega$. The sensitivity can be analyzed between any two equivalent resistance values (representative of the resistances before and binding to the agent) in the same manner as the analysis presented for Figure 9(a).

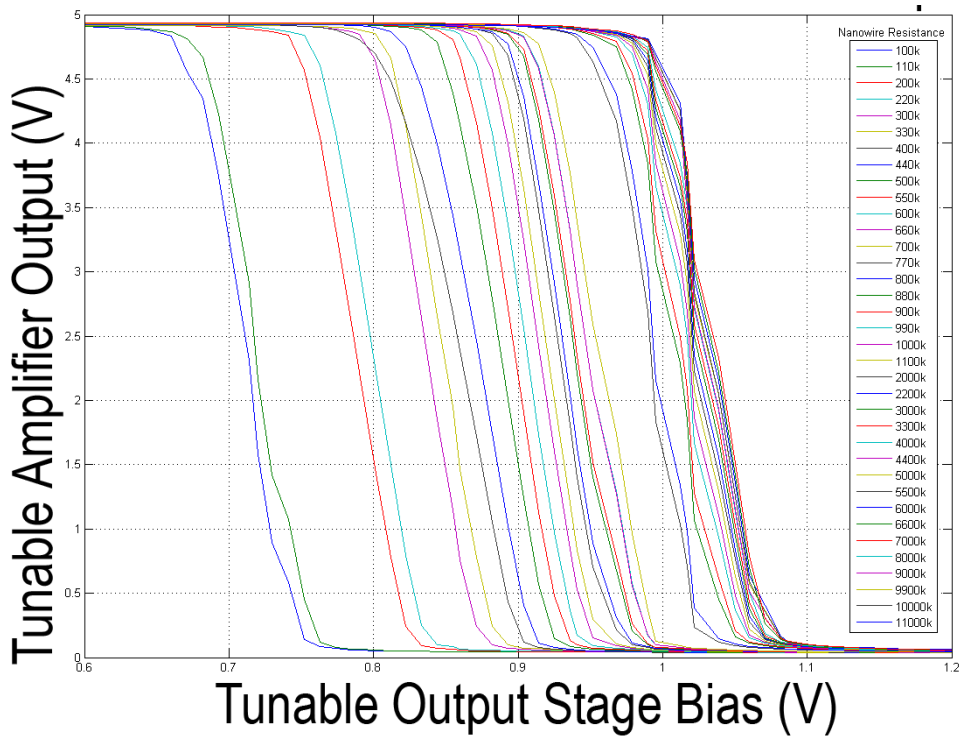
VII. CONCLUSIONS

Development of the technology to produce a low-cost, portable method of detecting biological and chemical agents (pathogens, toxins, etc.) in real time has vast ethical and societal impact. This lab-on-a-chip device has applicability in health and defense industries, providing a means to test samples for pathogens in a matter of minutes, as opposed to several hours. The size and relatively small number of components on the chip allows for quick and inexpensive deployment in both the field and laboratory settings. The limiting factor then becomes obtaining a solution of nanowires characterized to the specific pathogen one would like to detect, which is a design-dependent parameter. In the presented prototype, the types of pathogens that lead to resistivity changes in the $100\text{k}\Omega$ to $100\text{M}\Omega$ range are considered.

Comparison of Simulated and Fabricated CMOS Sensor ASIC Output versus Applied Bias



(a) Simulated vs. measured values of the IC sensor output with the tunability range for 500kΩ and 550kΩ nanowires.



(b) Measured output voltage vs. bias voltage of the tunable stage (i.e. IC sensor output) with the tunability range for various nanowire resistances.

Fig. 9. Simulated and measured sensitivity curves at the tunable amplifier output for varying equivalent resistance of nanowires.

The presented AIMS system is designed with an embedded PCB board for data acquisition. In the future, all components can be embedded on the lab-on-the-chip for increased portability. The presented lab-on-a-chip IC component is of $1.5 \times 1.5 \text{ mm}^2$ size, dissipates 120 mW on average and boosts a settling time of $30 \mu\text{s}$ in a tunability range of $100\text{k}\Omega$ to $100\text{M}\Omega$ in nanowire resistance. The work presents a novel IC implementation for the proposed nanowire-based sensor platform. Further research is necessary in nanowire deposition techniques and detection resolution enhancement.

REFERENCES

- [1] Y. Cui and C. M. Lieber, "Functional nanoscale electronic devices assembled using silicon nanowire building blocks," *Science*, vol. 291, no. 5505, pp. 851–853, February 2001.
- [2] L. Cao, B. Garipcan, E. M. Gallo, S. S. Nonnenmann, B. Nabet, and J. E. Spanier, "Excitation of local field enhancement on silicon nanowires," *Nano Letters*, vol. 8, no. 2, pp. 601–605, 2008.
- [3] D. K. Ferry, "Nanowires in nanoelectronics," *Science*, vol. 319, no. 5863, pp. 579–580, February 2008.
- [4] Y. Cui, Q. Wei, H. Park, and C. M. Lieber, "Nanowire nanosensors for highly sensitive and selective detection of biological and chemical species," *Science*, vol. 293, no. 5533, pp. 1289–1292, Aug 2001.
- [5] F. Patolsky, G. Zheng, O. Hayden, M. Lakadamyali, X. Zhuang, and C. M. Lieber, "Electrical detection of single viruses," *PNAS*, vol. 101, no. 39, pp. 14 017–14 022, Sept. 2004.
- [6] J. Rich, B. Dickinson, J. Carney, A. Fisher, and R. Heimer, "Detection of HIV-1 nucleic acid and HIV-1 antibodies in needles and syringes used for non-intravenous injection," *AIDS*, vol. 12, no. 17, pp. 2345–2350, Nov. 1998.
- [7] Z. Fan and J. Lu, "Gate-refreshable nanowire chemical sensors," *Applied Physics Letters*, vol. 86, pp. 123 510–123 512, 2005.
- [8] E. Stern, J. Klemic, D. Routenberg, P. Wyrembak, D. Turner-Evans, A. Hamilton, D. LaVan, T. Fahmy, and M. Reed, "Label-free immunodetection with cmos-compatible semiconducting nanowires," *Nature (London)*, vol. 445, 2007.
- [9] J. Kong, N. Franklin, C. Zhou, M. Chapline, S. Peng, K. Cho, and H. Dai, "Nanotube molecular wires as chemical sensors," *Science*, vol. 287, pp. 622–625, 2000.
- [10] M. McAlpine, H. Ahmad, D. Wang, and J. Heath, "Highly ordered nanowire arrays on plastic substrates for ultrasensitive flexible chemical sensors," *Nature Materials*, vol. 6, pp. 379–384, 2007.
- [11] P. Chen, G. Shen, and C. Zhou, "Chemical sensors and electronic noses based on onedimensional metal oxide nanostructures," *IEEE Transactions Nanotechnology*, vol. 7, no. 6, pp. 668–682, November 2008.
- [12] H. Bruus, *Theoretical Microfluidics*. Oxford University Press, 2007.
- [13] K. E. Herold and A. Rasooly, Eds., *Lab on a Chip Technology: Fabrication and Microfluidics*. Caister Academic Press, 2009.
- [14] A. H. Pohl, *Dielectrophoresis the behavior of neutral matter in nonuniform electric fields*. Cambridge University Press, 1978.
- [15] R. J. Baker, *CMOS: Circuit Design, Layout, and Simulation*. Wiley-IEEE, 2010.
- [16] A. S. Sedra and K. C. Smith, *Microelectronic Circuits*. Oxford University Press, 2009.
- [17] J. Catsoulis, *Designing Embedded Hardware*, 2nd ed., A. Oram, Ed. O'Reilly, 2005.
- [18] *DS80C400 Network Microcontroller data sheet*, 7th ed., Dallas Semiconductor, Maxim, June 2009.
- [19] *CoolRunner-II CPLD Family data sheet*, 3rd ed., Xilinx, September 2008.
- [20] "Mosis website," <http://www.mosis.com/>, November 2010.

Kyle Yencha received the B.S. degree in computer engineering from Drexel University, Philadelphia, PA in 2009.

Matthew Zofchak received the B.S. and M. S. degrees in computer engineering and electrical engineering, respectively, from Drexel University, Philadelphia, PA in 2009.

Daniel Oakum received the B.S. degree in computer engineering from Drexel University, Philadelphia, PA in 2009.

Gerre Strait received the B.S. degree in electrical engineering from Drexel University, Philadelphia, PA in 2009.



Baris Taskin received the B.S. degree in electrical and electronics engineering with a minor in operations research from Middle East Technical University, Ankara, Turkey, in 2000, and the M.S. and Ph.D. degrees in electrical engineering from University of Pittsburgh, Pittsburgh, PA, in 2003 and 2005, respectively. He also received the certificate in system-on-chip (SOC) design from The Technology Collaborative (TTC), Pittsburgh, PA in 2003.

He joined the Department of Electrical and Computer Engineering, Drexel University, Philadelphia, PA, as an Assistant Professor in 2005. Between 2003–2004, he was a staff engineer at MultiGiG Inc., Scotts Valley, CA, working on electronic design automation of integrated circuit timing and clocking. He is the coauthor of the book entitled *Timing Optimization Through Clock Skew Scheduling* (Springer, 2009). His research interests include resonant clocking, circuit timing, high performance integrated circuits, and nanoarchitectures. He is a recipient of the Association for Computing Machinery (ACM) Special Interest Group on Design Automation (SIGDA) A. Richard Newton Award in 2007 and the National Science Foundation (NSF) Faculty Early Career Development (CAREER) Award in 2009.



Bahram Nabet received the B.S.E.E. degree (with honors) from Purdue University, West Lafayette, IN, in 1977 and the M.S.E.E. and Ph.D. degrees from the University of Washington, Seattle, in 1985 and 1989, respectively. He joined the faculty of Drexel University, Philadelphia, PA, in 1989, where he is currently a Professor of electrical and computer engineering, an Affiliated Professor of materials science and engineering, and an Associate Dean for Special Projects in the College of Engineering. He has been a Visiting Professor in Brazil and Italy and

has served as a Chief Technical Advisor to Dexxon Group in France. His areas of research include optoelectronics, reduced-dimensional systems such as quantum dots, nanowires and 2-D gas devices, and plasmonics.